Journal of Photochemistry and Photobiology A: Chemistry 310 (2015) 171–179

Contents lists available at ScienceDirect

Journal of Photochemistry and Photobiology A: Chemistry

journal homepage: www.elsevier.com/locate/jphotochem

# Synthesis, spectroscopic properties and photodynamic activity of a fulleropyrrolidine bearing a basic amino group and its dicationic analog against *Staphylococcus aureus*

Maximiliano L. Agazzi, Mariana B. Spesia, Natalia S. Gsponer, M. Elisa Milanesio, Edgardo N. Durantini*

*Departamento de Química, Facultad de Ciencias Exactas, Físico-Químicas y Naturales, Universidad Nacional de Río Cuarto, Agencia Postal Nro 3, X5804BYA Río Cuarto, Córdoba, Argentina*

ARTICLE INFO

*Article history:*
Received 3 January 2015
Received in revised form 30 April 2015
Accepted 17 May 2015
Available online 21 May 2015

*Keywords:*
Fullerene
Photosensitizer
Photodynamic inactivation
Bacteria
*Staphylococcus aureus*

ABSTRACT

*N*-Methyl-2-[4-(3-*N*,*N*-dimethylaminopropoxy)phenyl]fulleropyrrolidine ($MPC_{60}$) was synthesized by 1,3-dipolar cycloaddition reaction of 4-(3-*N*,*N*-dimethylaminopropoxy)benzaldehyde, *N*-methylglycine and fullerene $C_{60}$ in 43% yield. The amine groups of $MPC_{60}$ were methylated with dimethyl sulfate to obtain a dicationic fullerene $DPC_{60}^{2+}$ in 96 % yield. Absorption spectra of these fullerenes in *N*, *N*-dimethylformamide (DMF) and toluene/sodium bis(2-ethylhexyl) sulfosuccinate (AOT)/water reverse micelles showed strong absorptions in the UV region, with a peak at 430 nm and broader range of absorption up to 710 nm. Fluorescence quantum yields of about $10^{-4}$ were calculated for these compounds in DMF. A higher singlet molecular oxygen, $O_2(^1\Delta_g)$, generation was found for $MPC_{60}$ than $DPC_{60}^{2+}$ in DMF. The photodynamic activity of these photosensitizers remained high in a simple biomimetic AOT system. Also, the formation of superoxide anion radical induced by $MPC_{60}$ and $DPC_{60}^{2+}$ was detected in presence of NADH. Decomposition of L-tryptophan in DMF mediated by both fullerenes indicated a possible contribution of type I photoprocess. Photosensitized inactivation of *Staphylococcus aureus* was investigated using different conditions. Cell suspensions of $10^8$ cells/mL incubated with 0.5 μM fullerene and irradiated for 30 min exhibited a 4.4 and 5.0 log decrease of cell survival by $MPC_{60}$ and $DPC_{60}^{2+}$, respectively. Therefore, these fullerene derivatives can be used as effective photosensitizers for the photodynamic inactivation of *S. aureus* cells.



## 1. Introduction

In recent years, new approaches to the treatment of microbial infections have become necessary due to the changing patterns of infectious diseases and the emergence of antibiotic-resistant microbes. This is mainly because of the inappropriate prescription of antibiotics, the application in prophylaxis and the systemic use that also affect the normal flora and the failure of patients to complete the treatments. The antibiotic era was perhaps largely expected to eliminate *Staphylococcus aureus* and other bacterial pathogens as a leading cause of human infections [1]. However, *S. aureus* has extraordinary ability to develop resistance to antibiotics, which have been the impetus for waves of antimicrobial resistance over the past 60 years [2]. In this sense, new alternative therapies have been proposed [3]. In particular, photodynamic inactivation (PDI) of microorganisms has been proposed to controlling bacterial infections [4]. PDI involves the administration of a photosensitizer that is accumulated in the microbial cells and the subsequent irradiation with visible light. In the presence of oxygen, the photodynamic activity produces cell inactivation. The main advantages of this approach are: (i) fast eradication of microorganisms, (ii) double selectivity, specific accumulation of photosensitizer in microbial cells and light delivered only to affected area and (iii) similar photoinactivation regardless of the antibiotic resistance and lack of induction of resistance to photodynamic treatments [5].

Appropriate photosensitizers have specific chemical and biological properties. Thus, the combination of visible light absorption and a long lifetime of triplet excited state allow fullerenes to act as photosensitizers [6]. However, fullerenes are hydrophobic molecules with low solubility in polar solvents and consequently fullerenes form aggregates in aqueous solutions [7]. Thus, the lack of solubility in biological environments is the major obstacle in the development of this field. Different approaches

* Corresponding author. Tel.: +54 358 4676157; fax: +54 358 4676233.
*E-mail address:* edurantini@exa.unrc.edu.ar (E.N. Durantini).

http://dx.doi.org/10.1016/j.jphotochem.2015.05.022
1010-6030/

have been developed for the transfer of fullerenes to water. Perhaps, the most versatile methodology to resolve this problem is based on the chemical modification of the fullerene by the attachment of functional hydrophilic cationic groups. These amphiphilic fullerenes can produce an increase in the biological activity and therefore act as efficient photosensitizer to inactivate microbial cells. The development of covalent chemistry of $C_{60}$ has opened the possibility to attach this sphere structure with several groups, which allows increase in the biological activity [8]. Thus, chemical modification of the fullerene can be used to attach functional hydrophilic cationic groups. These amphiphilic fullerenes can be efficient photosensitizer in biological media. Interesting results using cationic fullerenes as photosensitizers have been found to photoinactivate microorganisms [9–11].

Under aerobic conditions, the triplet excited state of fullerene ($^3C_{60}^*$) can interact with ground state molecular oxygen to form reactive oxygen species (ROS). This process can occur by energy transfer from the $^3C_{60}^*$ to produce singlet molecular oxygen, $O_2(^1\Delta_g)$ or by electron transfer to form superoxide anion radical ($O_2^{\bullet-}$) [12]. Fullerenes are extremely efficient $O_2(^1\Delta_g)$ generators with a quantum yield that is near unity. On the other hand, fullerenes can be easily reduced to $C_{60}$ radical anion ($C_{60}^{\bullet-}$) by electron transfer. Thus, the $^3C_{60}^*$ or $C_{60}^{\bullet-}$ can transfer an electron to molecular oxygen forming $O_2^{\bullet-}$. In contrast to $O_2(^1\Delta_g)$ generation, the electron transfer type of reaction preferentially occurs in polar solvents, particularly in the presence of reducing agents such as NADH. These pathways, yielding $O_2(^1\Delta_g)$ and $O_2^{\bullet-}$, are analogous to the two main photochemical reaction types known as type II and type I mechanisms, respectively [6].

In the present work, a novel fulleropyrrolidine $C_{60}$ derivative ($MPC_{60}$) was synthetized, which contains an aliphatic chain with an amino group at the end (Scheme 1). The nitrogen atoms in the amine groups were used to obtain a dicationic fulleropyrrolidinium ($DPC_{60}^{2+}$). The formation of cationic amphiphilic photosensitizers has several interesting features that make these compounds attractive photosensitizers for a variety of biological systems [6]. The spectroscopic and photodynamic properties of these fullerenes were studied in organic solution and in a simple biomimetic medium formed by reverse micellar system. Also, photodynamic activity mediated by these photosensitizers was evaluated *in vitro* for inactivation of *S. aureus* cells.

## 2. Materials and methods

### 2.1. General

Proton nuclear magnetic resonance spectra were performed on a FT-NMR Bruker Avance DPX400 spectrometer at 400 MHz. Mass spectra were recorded on a Bruker micrOTOF-QII (Bruker Daltonics, MA, USA) equipped with an atmospheric pressure photoionization (APPI) source. Absorption and fluorescence spectra were carried out in a Shimadzu UV-2401PC spectrometer (Shimadzu Corporation, Tokyo, Japan) and on a Spex FluoroMax spectrofluorometer (Horiba Jobin Yvon Inc., Edison, NJ, USA), respectively. Experiments of photooxidation of substrates were carried out with a Cole-Parmer illuminator 41,720-series (Cole-Parmer, Vernon Hills, IL, USA) with a 150 W halogen lamp through a high intensity grating monochromator (Photon Technology Instrument, Birmingham, NJ, USA). The visible light source used to irradiate cell suspensions was a Novamat 130 AF (Braun Photo Technik, Nürnberg, Germany) slide projector containing a 150 W lamp. A 2.5 cm glass cuvette filled with water was used to remove the heat from the lamp. A wavelength range between 350 and 800 nm was selected by optical filters. The fluence rate was determined as was 90 mW/cm$^2$ (Radiometer Laser Mate-Q, Coherent, Santa Clara, CA, USA).

All the chemicals from Aldrich (Milwaukee, WI, USA) were used as received. Sodium bis(2-ethylhexyl) sulfosuccinate (AOT) from Sigma (St. Louis, MO, USA) was dried under vacuum. Tetrasodium 2,2′-(anthracene-9,10-diyl) bis(methylmalonate) (ABMM) was synthetized as previously described (13). Silica gel thin-layer chromatography (TLC) Plates 250 microns from Analtech (Newark, DE, USA) were used. Solvents (GR grade) from Merck (Darmstadt, Germany) were distilled. Labconco (Kansas, MO, USA) equipment model 90,901-01 was used to obtain ultrapure water.

### 2.2. Synthesis of fullerene $C_{60}$ derivatives

*N*-Methyl-2-[4-(3-*N*,*N*-dimethylaminopropoxy)phenyl]fulleropyrrolidine ($MPC_{60}$). A solution of $C_{60}$ (51 mg, 0.071 m mol), 4-(3-*N*,*N*-dimethylaminopropoxy) benzaldehyde (25 mg, 0.120 mmol) and *N*-methylglycine (26 mg, 0.292 mmol) in 55 mL of dry toluene was stirred at reflux under an argon atmosphere for 6 h. Then, the solvent was removed under vacuum. Flash column chromatography (silica gel) using toluene/ethyl acetate (100:0–50:50 gradient, 1% triethylamine) as eluent afforded 29 mg (43%) of $MPC_{60}$. TLC (sílica gel, toluene/ethyl acetate/triethylamine, 1:1:0.01) $R_f$ = 0.2. $\lambda_{max}$ (DMF) [nm] ($\varepsilon$, M$^{-1}$ cm$^{-1}$) 431 (3980). $^1$HNMR ($CDCl_3$, TMS) $\delta$ [ppm] 1.97 (m, 2H, —$CH_2$—), 2.28 (s, 6H, N($CH_3$)$_2$), 2.50 (t, 2H, $NCH_2$—, $J$ = 7.0 Hz), 2.79 (s, 3H, $NCH_3$ pyrrolidine ring), 4.02 (t, 2H, $OCH_2$—, $J$ = 6.1 Hz), 4.24 (d, 1H, pyrrolidine ring, $J$ = 9.4 Hz), 4.88 (s, 1H, pyrrolidine ring); 4.97 (d, 1H, pyrrolidine ring, $J$ = 9.4 Hz), 6.95 (d, 2H, Ar, $J$ = 8.0 Hz), 7.70 (d, 2H, Ar, $J$ = 8.0 Hz). APPI-MS [$m/z$] 955.1810 [M + H]$^+$ (954.1732 calculated for $C_{74}H_{22}N_2O$).

*N*,*N*-Dimethyl-2-[4-(3-*N*,*N*,*N*-trimethylammoniopropoxy)phenyl]fulleropyrrolidinium ($DPC_{60}^{2+}$). A mixture of $MPC_{60}$ (10 mg, 0.010 mmol) and dimethyl sulfate (200 μL, 2.11 mmol) in 2 mL of *N*,*N*-dimethylformamide (DMF) was stirred for 40 h at 90 °C under an

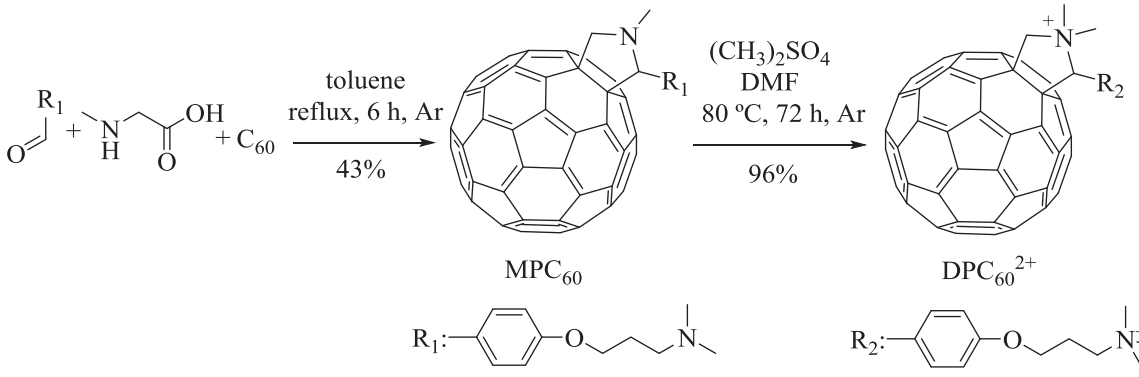


**Scheme 1.** Synthesis of fullerene derivatives.

argon atmosphere. The solvent was removed under vacuum and the mixture was placed in Eppendorf tubes and ethyl ether was added. The methylated product was precipitated. It was washed with 5% aqueous $Na_2CO_3$ and then with water to obtain 96% of $DPC_{60}^{2+}$. $\lambda_{max}$ (DMF) [nm] ($\varepsilon$, $M^{-1}\,cm^{-1}$) 431 (3920). $^1H$ NMR ($CS_2$/acetone-$d_6$, TMS) δ [ppm] 2.40 (m, 2H, —$CH_2$—), 3.28 (s, 9H, $N^+(CH_3)_3$), 3.32 (t, 2H, $NCH_2$—, $J$ = 6.9 Hz), 3.88 (s, 6H, $N^+(CH_3)_2$ pyrrolidine ring), 4.00 (t, 2H, $OCH_2$—$J$ = 6.0 Hz), 4.30 (d, 1H, pyrrolidine ring, $J$ = 9.5 Hz), 4.94 (s, 1H, pyrrolidine ring); 5.02 (d, 1H, pyrrolidine ring, $J$ = 9.5 Hz), 6.92 (d, 2H, Ar, $J$ = 8.0 Hz), 7.69 (broad signal, 2H, Ar). APPI-MS [$m/z$] 985.2280 $[M+H]^+$ (984.2202 calculated for $C_{76}H_{28}N_2O$).

### 2.3. Spectroscopic studies

Absorption and fluorescence spectra were performed in a quartz cell of 1 cm path length using DMF, toluene and toluene/AOT (0.1 M)/water ($W_0$ = 10) media at 25.0 ± 0.5 °C. Absorbances <0.05 were matched at the excitation wavelength (450 nm) and the areas of the emission spectra were integrated in the range 600–800 nm. The fluorescence quantum yield ($\Phi_F$) of fullerenes were calculated by comparison of the area below the corrected emission spectrum with that of $C_{60}$ as a reference ($\Phi_F = 2.3 \times 10^{-4}$), exciting at $\lambda_{exc}$ = 450 nm in DMF [10]. AOT reverse micelles were prepared from a stock solution of 0.1 M AOT, which was prepared by weighing and dilution in toluene. The amount of water dispersed in the system was reported as the molar ratio between water and the AOT present in the reverse micelle ($W_0 = [H_2O]/[AOT]$). In all experiments, $W_0$ = 10 was used and the mixtures were sonicated for about 10 s to obtain perfectly clear micellar system [14].

### 2.4. Steady state photolysis

Photooxidation of 1,3-diphenylisobenzofuran (DPBF). Solutions of DPBF (20 μM) and fullerene in DMF were irradiated in 1 cm path length quartz cells (2 mL) with monochromatic light at $\lambda_{ir}$ = 480 nm (fullerene absorbance 0.1). The light fluence rate was determined as 0.60 mW/cm$^2$. The photooxidation of DPBF was studied by following the decrease of the absorbance at $\lambda_{max}$ = 415 nm. After irradiation, the formation of products interfering in the absorption spectra was not detected and the absorption due to fullerene derivatives was unchanged. Thus, the absorption changes can be assigned to the photooxidation of DPBF mediated by fullerenes.

Photooxidation of 9,10-dimethylanthracene (DMA) and ABMM. Solutions of anthracene derivative (35 μM) and fullerene in different media (DMA in DMF or AOT micelles and ABMM in water or DMF/water 1:1) were irradiated as described for DPBF using $\lambda_{irr}$ = 450 nm (light fluence 0.45 mW/cm$^2$). Antracene photodecomposition was monitored following the decrease in absorbance at $\lambda_{max}$ = 378 nm.

Quantum yields of $O_2(^1\Delta_g)$ production ($\Phi_\Delta$). The observed rate constants ($k_{obs}$) of DPBF or DMA photodecomposition were obtained by a linear least-squares fit of the semilogarithmic plot of ln ($A_0/A$) *vs*. time. Values of $\Phi_\Delta$ in DMF were calculated comparing the $k_{obs}$ for the corresponding fullerene with that for $C_{60}$, which was used as a reference ($\Phi_\Delta$ = 1) [15,16]. Measurements of the sample and reference under the same conditions afforded $\Phi_\Delta$ for photosensitizers by direct comparison of the slopes in the linear region of the plots.

Photooxidaion of nitro blue tetrazolium (NBT). The NBT method was used to detect superoxide anion radical ($O_2^{\bullet-}$) formation in DMF [17,18]. The NBT method was carried out using 0.2 mM NBT, 0.5 mM NADH and fullerene (10 μM) in 2 mL of DMF. Control experiments were performed in absence of NBT, NADH or fullerene. Samples were irradiated in 1 cm path length quartz cells under aerobic condition with visible light filtered through a 2.5 cm glass cuvette filled with water (light fluence 44 mW/cm$^2$). The progress of the reaction was monitored by following the increase of the absorbance at λ = 560 nm.

Photooxidation of L-tryptofan (Trp). Solutions of Trp (20 μM) and fullerene in DMF were treated as described above for photodecomposition of DMA. Photooxidation of Trp were studied by following the decrease of the fluorescence intensity at λ = 350 nm, exciting the samples at $\lambda_{exc}$ = 290 nm. Control experiments showed that under these conditions the fluorescence intensity correlates linearly with Trp concentration. The observed rate constants ($k_{obs}$) were obtained by a linear least-squares fit of semi-logarithmic plots of ln ($F_0/F$) vs. time.

### 2.5. Bacterial strain and preparation of cultures

The Gram-positive strain *S. aureus* ATCC 25,923 was used in this study. This bacterium was grown on a rotator shaker (100 rpm) at 37 °C in tryptic soy (TS, Britania, Buenos Aires, Argentina) broth overnight. An aliquot (60 μL) of this culture was aseptically transferred to 4 mL of fresh medium (TS broth) and incubated at 37 °C to mid logarithmic phase of growth (absorbance ∼0.3 at 660 nm). After that, cells were harvested by centrifugation of broth cultures (3000 rpm for 15 min) and re-suspended in 4 mL of 10 mM phosphate-buffered saline (PBS, pH 7.0). Then the cells were diluted 1/1000 or 1/10 in PBS, corresponding to ∼$10^6$ and ∼$10^8$ colony forming units (CFU)/mL, respectively.

### 2.6. Photosensitized inactivation of bacteria cells

Cell suspensions of *S. aureus* (2 mL, ∼$10^6$ CFU/mL or ∼$10^8$ CFU/mL) in PBS were incubated with 0.5 μM fullerene in Pyrex culture tubes (13 × 100 mm) for 30 min in the dark at 37 °C. Photosensitizers were added from a stock solution in DMF (0.5 mM). Then, two protocols were followed: (a) 2 mL of ∼$10^6$ CFU/mL were directly irradiated in Pyrex culture tubes and (b) 0.2 mL of ∼$10^8$ CFU/mL were placed in each well of 96-well microtiter plates (Deltalab, Barcelona, Spain). In both cases, the cultures were exposed for different time intervals to visible light using the irradiation system described in section 2.1. Serial dilutions of irradiated cell suspensions and controls were performed with PBS and each sample was plated in triplicate on TS agar. The number of colonies formed after ∼24 h incubation at 37 °C was counted.

### 2.7. Controls and statistical analysis

Control experiments were performed in presence and absence of fullerene in the dark and in the absence of photosensitizer with cells irradiated. The amount of DMF used in each experiment was not toxic to *S. aureus* cells. Three values were obtained per each condition and each experiment was repeated separately three times. The unpaired *t*-test was used to establish the significance of differences between groups. Differences were considered statistically significant with a confidence level of 95% ($p < 0.05$). Data were represented as the mean ± standard deviation of each group.

## 3. Results and discussion

### 3.1. Synthesis of fullerene derivatives

The synthetic procedures to obtain fullerene derivatives are briefed in Scheme 1. First, $MPC_{60}$ was obtained by 1,3-dipolar cycloaddition reaction in dry toluene using 4-(3-*N*,*N*-dimethylaminopropoxy) benzaldehyde, *N*-methylglycine and fullerene $C_{60}$, (1.7:4.1:1.0) molar relationship, respectively. The solution was stirred for 6 h at reflux in an argon atmosphere. This reaction

mixture produced $MPC_{60}$, which was purified by flash chromatography (silica gel) giving 43% yield. Thus, the synthesis of $MPC_{60}$ was performed on the base of fulleropyrrolidine formation developed by Prato et al. [19]. Similar fulleropyrrolidine bearing a flexible attachment with an *N*-methylaniline end group was previously prepared [20]. The amine groups in the structure of $MPC_{60}$ were the precursor of a dicationic $DPC_{60}^{2+}$ by methylation. Thus, $DPC_{60}^{2+}$ was formed treating $MPC_{60}$ with an excess of dimethyl sulphate for 72 h at 80 °C. The exhaustive methylation produced $DPC_{60}^{2+}$ in high yields (96%).

The structure of $DPC_{60}^{2+}$ is formed by a hydrophobic carbon sphere containing two cationic groups that provide an amphiphilic character. The mainly difference between both fullerenes is the presence of two intrinsic cationic charges in $DPC_{60}^{2+}$ in contrast with $MPC_{60}$, which is substituted by an aliphatic amine group. This basis amine group in the periphery of $MPC_{60}$ could acquire positive charges, depending on the medium in which the fullerene is located. Moreover, in these structures the cationic center is isolated from the fullerene by a propoxy bridge. Thus, this charge has minimal influence on the electronic density of the sphere. This helps to retain the consistency of the photophysical properties of the fullerene. Also, this chain provides a higher mobility of the charge, which could facilitate the interaction with the membrane of the bacteria.

### 3.2. Absorption and fluorescence spectroscopic studies

UV–visible absorption spectra of $MPC_{60}$ and $DPC_{60}^{2+}$ in DMF, toluene and toluene/AOT (0.1 M)/water ($W_0 = 10$) are shown in Fig. 1. These fullerenes had moderately strong $\pi$–$\pi^*$ absorption bands in the UV region. In the visible region, a broader range of absorption up to almost 710 nm was observed with a sharp peak at 430 nm. Also, a very weak broader band characteristic of $C_{60}$ derivatives was detected at 707 nm for $MPC_{60}$ and at 708 nm for $DPC_{60}^{2+}$ in DMF [21]. Monofunctionalization of the fullerene core influences the electronic structure and leads to a change of the $I_h$-symmetry of pristine $C_{60}$, which adapts an effective $C_{2v\times}$ symmetry [20]. On the other hand, similar shapes in the $MPC_{60}$ absorption spectra were found in the organic solvents and in AOT micelles indicating a solubilization mainly as monomer in these media. In contrast, a low intensity and a broadening of the bands were observed in the spectrum of $DPC_{60}^{2+}$ in toluene due to aggregation of the dicationic fullerene in this non-polar medium (Fig. 1). However, the spectrum intensity of $DPC_{60}^{2+}$ increases in toluene/AOT/water, indicating that this micellar system helps the solubilization of cationic fullerene as monomer.

The steady-state fluorescence emission spectra of $MPC_{60}$ and $DPC_{60}^{2+}$ were compared with that of $C_{60}$ in DMF exciting the samples at 450 nm (Fig. 2). The spectra showed a band centered at 717 nm for $MPC_{60}$ and 716 nm for $DPC_{60}^{2+}$, which are characteristic for similar fulleropyrrolidines [10,22]. The fluorescence spectrum of *N*-methylfulleropyrrolidine is in agreement with the mirror imaged absorption features [22]. This reflects the fact that the force constants of vibrational levels in the first singlet excited state resemble those in the singlet ground state. The good match of the longest-wavelength absorption and the shortest wavelength emission and the fact that they exhibit the highest oscillator strengths are convincing evidence for an assignment to $0^* \rightarrow 0$ transition bands. From the intersection of the absorption and fluorescence spectra, Stokes shifts of ~10 nm were calculated for these fullerenes. These Stokes shifts indicated that in these molecules the spectroscopic energies are similar to the relaxed energies of the lowest singlet excited state $S_1$, according to the rigid structure of the fullerenes. That suggests that only a minor geometric relaxation occurs in the first excited state. Since the energy of the 0-0 electronic transitions, the energy levels of the singlet excited stated ($E_s$) were calculated giving in both cases a value of 1.74 eV. This $E_s$ value is similar to those previously reported for this kind of fullerene derivatives [22]. Values of $\Phi_F$ for these photosensitizers were calculated by comparison with $C_{60}$ as a reference in the $S_1$ state in DMF, giving $(5.2 \pm 0.5) \times 10^{-4}$ and $(2.8 \pm 0.3) \times 10^{-4}$ for $MPC_{60}$ and $DPC_{60}^{2+}$, respectively. In general, fullerene $C_{60}$ derivatives present a low fluorescence emission and these values agree with those previously reported by similar fullerenes [23,24].

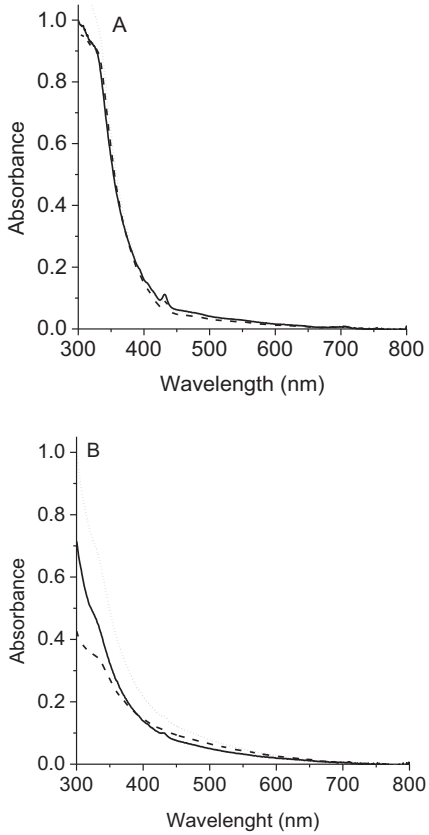


**Fig. 1.** Absorption spectra of (A) $MPC_{60}$ and (B) $DPC_{60}^{2+}$ in DMF (solid line), toluene (dashed line) and toluene/AOT (0.1 M)/water ($W_0 = 10$) (dotted line).

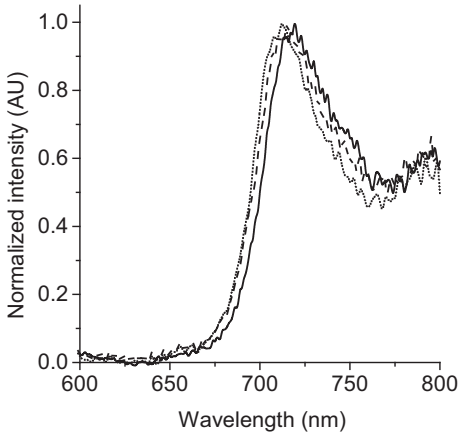


**Fig. 2.** Fluorescence emission spectra of $MPC_{60}$ (solid line), $DPC_{60}^{2+}$ (dashed line) and $C_{60}$ (dotted line) in DMF, $\lambda_{exc} = 450$ nm.

### 3.3. Photodynamic activity

#### 3.3.1. Photooxidation of DPBF

The photooxidation of DPBF induced by fullerene derivatives was studied in DMF. DPBF is decomposed by $O_2(^1\Delta_g)$ generated to produce 1,2-dibenzoylbenzene [25]. Thus, this substrate was used to evaluate the ability of the fullerenes to produce $O_2(^1\Delta_g)$. A time-dependent decrease in the DPBF concentration was observed by following a decrease in its absorbance at 415 nm (Fig. 3). From first-order kinetic plots the values of the observed rate constant ($k_{obs}$) were calculate for DPBF. The results are shown in Table 1. Values of $\Phi_\Delta$ were calculated comparing the slope for $MPC_{60}$ and $DPC_{60}^{2+}$ with the corresponding slope obtained for the reference, $C_{60}$. $MPC_{60}$ and $C_{60}$, photodecompose DPBF with comparable rates, indicating that $O_2(^1\Delta_g)$ was efficiently produced by $MPC_{60}$ in this medium. Similar results of $O_2(^1\Delta_g)$ production were previously found a non-charged *N*-methyl-2-(4′-acetamidophenyl) fulleropyrrolidine in DMF/water (10%) [10]. Therefore, introduction of a substituent on fullerene core produced a decrease in the photodynamic activity. On the other hand, photodecomposition of DPBF photosensitized by $DPC_{60}^{2+}$ was lower than that of $MPC_{60}$. In previous studies it was found a very low of $\Phi_\Delta$ for *N*,*N*-Dimethyl-2-(4′-*N*,*N*,*N*-trimethylaminophenyl) fulleropyrrolidinium due to an incomplete monomerization of the dicationic fullerene in DMF/water (10%) [10]. However, for $DPC_{60}^{2+}$ showed a $O_2(^1\Delta_g)$ production about half of that obtained for $MPC_{60}$.

#### 3.3.2. Photosensitized decomposition of DMA and ABMM

Photooxidation of anthracene derivatives induced by these photosensitizers was compared in different media under aerobic conditions. Fig. 4 shows characteristic semilogarithmic plots describing the progress of the reaction for DMA. Values of $k_{obs}^{DMA}$ were calculated from first-order kinetic plots of the DMA absorption at 378 nm with irradiation time (Table 1). In DMF, $MPC_{60}$ efficiently induced the decomposition of DMA, whereas lower reaction rate was detected using $DPC_{60}^{2+}$ as photosensitizer (Fig. 4A). Moreover, the kinetic data of DMA decomposition were used to estimate the $\Phi_\Delta$ values considering that this substrate quenches $O_2(^1\Delta_g)$ by chemical reaction [25]. As can be observed in Table 1, comparable values of $\Phi_\Delta$ were obtained for fullerenes using DMA or DPBF, which are quite reasonable values for monosubstituted fullerenes dissolved as monomers [16].

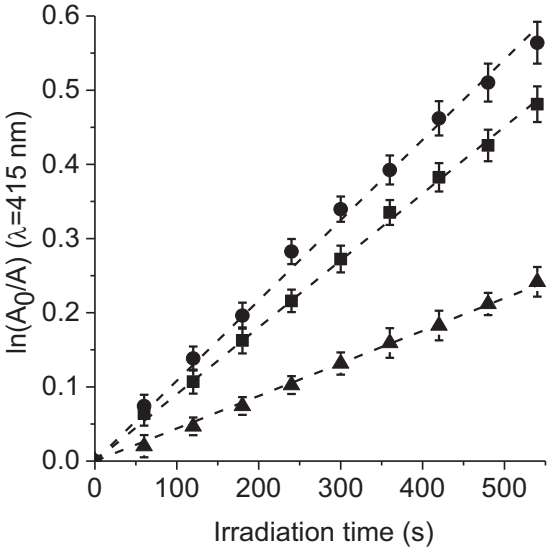


**Fig. 3.** First-order plots for the photooxidation of DPBF (20 μM, $\lambda_{irr}$ = 480 nm) photosensitized by $C_{60}$ (●), $DPC_{60}$ (■) and $DPC_{60}^{2+}$ (▲) in DMF. Values represent mean ± standard deviation of three separate experiments.

ABMM was used as a molecular probe for the detection of $O_2(^1\Delta_g)$ in aqueous solution [13]. Photooxidation of this substrate mediated by fullerenes was not detected in water after 10 min irradiation. These fullerenes can form aggregates in this medium, producing a considerable decrease in the formation of $O_2(^1\Delta_g)$ [10]. Photodecomposition of ABMM was detected in DMF/water (1:1).

As shown in Table 1, a lower value of $k_{obs}^{ABMM}$ was found using $DPC_{60}^{2+}$ than $MPC_{60}$. A difficulty of ABMM anionic trap is the interaction with cationic photosensitizers [13]. The interaction of ABMM with $DPC_{60}^{2+}$ can be interfering in the $O_2(^1\Delta_g)$ generation.

Moreover, photooxidation of DMA mediated by fullerenes was performed in toluene/AOT (0.1 M)/water ($W_0$ = 10) reverse micelles under aerobic conditions (Fig. 4B). This microheterogeneous system has been used as a simple biomimetic model of water pockets found in bioaggregates [26]. In micellar systems, a solute can be located in the organic solvent, the dispersed water pool or at the micellar interface [13]. Thus, compounds of different polarities can be dissolved simultaneously in reverse micelles. Photodecomposition of DMA by $O_2(^1\Delta_g)$ takes place in the toluene pseudophase where this non-polar molecule is mainly solubilized [13]. As shown in Table 1, a high $O_2(^1\Delta_g)$ generation was found for $MPC_{60}$ and $DPC_{60}^{2+}$. These fullerenes can interact with the AOT micelles through their substituents. Also, due to the high lipophilic character of the fullerene sphere, it is expected that fullerene is located at the micellar interface with the moiety of the $C_{60}$ situated at the nonpolar solvent. Localization of $C_{60}$ in the toluene pseudophase decrease the formation of type I reaction, favoring the photosensitization of $O_2(^1\Delta_g)$ from the fullerene triplet state. On the other hand, the reaction rates of DMA sensitized by fullerenes in the AOT micellar system were slower than those found in DMF (Table 1). Similar behavior was previously observed in AOT reverse micelles using porphyrins as photosensitizers [13]. In the AOT micellar system, $O_2(^1\Delta_g)$ is partitioned between the internal and external pseudophases. Also, the reaction rate of DMA photooxidation can be lower in the toluene pseudophase than in a more polar solvent, such as DMF [27].

#### 3.3.3. Photosensitized reduction of NBT

Generation of $O_2^{\bullet-}$ by $MPC_{60}$ and $DPC_{60}^{2+}$ was observed using NBT reduction to diformazan in presence of NADH, following the absorption at 560 nm in DMF (Fig. 5). Photosensitized decomposition of NBT ocurrs predominantly through a type I photoreaction process [17]. The increase in diformazan absorption was investigated as a function of time after irradiation with visible light. As can be observed in Fig. 5, reduction of NBT by $O_2^{\bullet-}$ was not found in the photoirradiated samples without NADH. Decomposition of NBT significantly increases in presence of $MPC_{60}$ or $DPC_{60}^{2+}$ and NADH after irradiation with respect to solution without the fullerenes. Therefore, even though $O_2(^1\Delta_g)$ can be generated effectively by photoexcited triplet state of fullerenes, it was observed that $O_2^{\bullet-}$ can also be produced in the presence of NADH. However, the biological microenvironment of the photosensitizer can produce important modifications in the photophysics of the fullerene derivatives established in solution.

#### 3.3.4. Photooxidation of Trp

Photosensitized decomposition of Trp was investigated in DMF. Trp can be photooxidized by both type I and type II reaction mechanisms and this amino acid can be a potential target of the ROS generated by fullerenes in cells [28,29]. As shown in Fig. 6, the photooxidation followed first-order kinetics with respect to Trp concentration. From the plots in Figure 6, the values of the $k_{obs}^{Trp}$ were determined for Trp decomposition. Table 1 shows that high photooxidation rates of Trp were obtained using these fullerenes as

**Table 1**
Kinetic parameters for the photooxidation reaction of DPBF ($k_{obs}^{DPBF}$), DMA ($k_{obs}^{DMA}$), and Trp ($k_{obs}^{Trp}$) and singlet molecular oxygen quantum yield ($\Phi_\Delta$) in different media.

| Parameters | Media | $C_{60}$ | $MPC_{60}$ | $DPC_{60}^{2+}$ |
|---|---|---|---|---|
| $k_{obs}^{DPBF}$ ($s^{-1}$) | DMF | $(1.08 \pm 0.03) \times 10^{-3}$ | $(0.90 \pm 0.02) \times 10^{-3}$ | $(0.45 \pm 0.02) \times 10^{-3}$ |
| $\Phi_\Delta$[a] | DMF | 1[e] | $0.83 \pm 0.04$ | $0.42 \pm 0.03$ |
| $k_{obs}^{DMA}$ ($s^{-1}$) | DMF | $(3.83 \pm 0.06) \times 10^{-5}$ | $(2.94 \pm 0.05) \times 10^{-5}$ | $(1.69 \pm 0.04) \times 10^{-5}$ |
| $\Phi_\Delta$[b] | DMF | 1[e] | $0.76 \pm 0.04$ | $0.44 \pm 0.03$ |
| $k_{obs}^{ABMM}$ ($s^{-1}$) | DMF/water[c] | – | $(2.30 \pm 0.06) \times 10^{-5}$ | $(1.40 \pm 0.05) \times 10^{-5}$ |
| $k_{obs}^{DMA}$ ($s^{-1}$) | AOT[d] | $(1.26 \pm 0.07) \times 10^{-5}$ | $(1.97 \pm 0.08) \times 10^{-5}$ | $(0.54 \pm 0.03) \times 10^{-5}$ |
| $k_{obs}^{Try}$ ($s^{-1}$) | DMF | – | $(1.12 \pm 0.04) \times 10^{-4}$ | $(0.79 \pm 0.03) \times 10^{-4}$ |

[a] From DPBF.
[b] From DMA.
[c] 1:1.
[d] Toluene/AOT (0.1 M)/water ($W_0 = 10$).
[e] From Ref. [15].

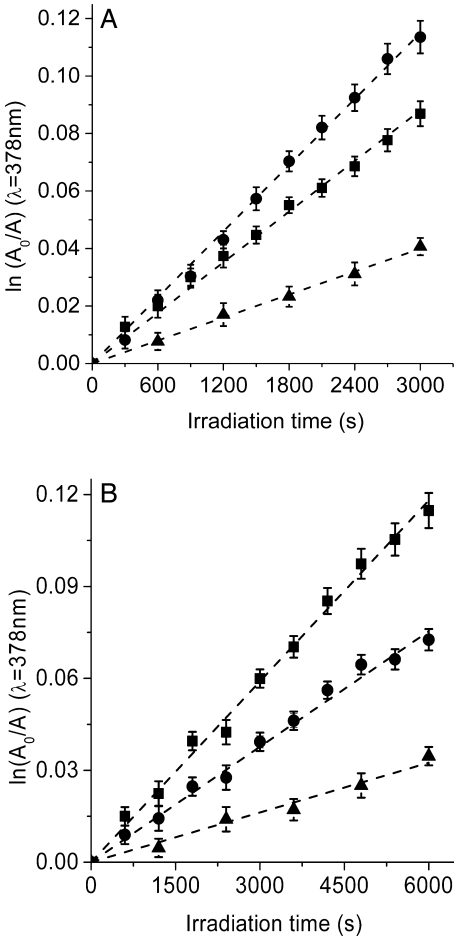


**Fig. 4.** First-order plots for the photooxidation of DMA (35 μM, $\lambda_{irr}$ = 450 nm) photosensitized by $C_{60}$ (●), $DPC_{60}$ (■) and $DPC_{60}^{2+}$ (▲) in (A) DMF and (B) toluene/AOT (0.1 M)/water ($W_0 = 10$). Values represent mean ± standard deviation of three separate experiments.

photosensitizers. The deactivation of fullerenes by an energy transfer mechanism to Trp can be ruled out on energetics grounds ($E_s$ = 1.77 eV for fullerenes; $E_s$ = 3.51 eV for Trp [30]) and due to the lack of appropriate spectral properties [31]. Possibly, interactions between these fullerenes and Trp can be favoring an electron transfer process in the decomposition of Trp. Also, the photosensitized oxidation of Trp was found to be more than two orders of magnitude more efficient *via* electron transfer than *via* $O_2(^1\Delta_g)$ [28]. Therefore photoinduced electron transfer can be involved in the photooxidation. Comparing the kinetic results of Trp and DMA in DMF, it can be observed that the ratio $k_{obs}^{Trp}/k_{obs}^{DMA}$ takes values of 3.8 and 4.7 for $MPC_{60}$ and $DPC_{60}^{2+}$, respectively. These results can be compared with similar studies using porphyrins as photosensitizers [32,33]. For non-charged porphyrins, the photooxidation of Trp mainly follows a process type II with $k_{obs}^{Trp}/k_{obs}^{DMA}$ values of about 0.4. However, this ratio considerably increased when the Trp decomposition was photosensitized by the fullerenes. Therefore, an electron transfer pathway may also be contributing, together with type II photoprocess, to Trp decomposition in DMF.

### 3.4. In vitro *studies on S. aureus cells*

The photodynamic activity of $MPC_{60}$ and $DPC_{60}^{2+}$ was investigated *in vitro* using a Gram-positive bacterium, *S. aureus*. Photoinactivation studies were realized using ~$10^6$ and ~$10^8$ CFU/mL cell densities. The cell toxicity produced by these fullerenes was evaluated in the absence of light at different fullerene concentrations. No toxicity was found in ~$10^6$ CFU/mL cultures treated with 2.5 μM $MPC_{60}$ for 30 min in dark. However, this concentration of $DPC_{60}^{2+}$ was cytotoxic without irradiation. Similar bacteriostatic effects of cationic fullerene derivatives were previously observed on *E.* cells [10]. A regio isomer mixture of $C_{60}$-bis(*N*,*N*-dimethylpyrrolidinium inhibited *E. coli* growth and oxygen uptake caused by cells. This result indicated that the mechanism of the bacteriostatic effect of cationic fullerenes is the inhibition of energy metabolism [34]. Moreover, cationic fullerene derivatives with different number of positive charges were dark toxic to *S. aureus* [9,11]. Finally, no dark toxicity was found when cell cultures (~$10^6$ CFU/mL and ~$10^8$ CFU/mL) were treated with 0.5 μM $DPC_{60}^{2+}$ or $MPC_{60}$ and therefore it was selected for *in vitro* photodynamic studies.

Suspensions of *S. aureus* cells in PBS were treated with 0.5 μM $MPC_{60}$ and $DPC_{60}^{2+}$ for 30 min at 37 °C in dark and then cultures were irradiated with visible light. Figs. 7 and 8 show the survival curve of bacterial cells after different irradiations times. Control experiments showed that the viability of *S. aureus* was unaffected by illumination alone or by dark incubation with 0.5 μM the photosensitizer for 30 min. Therefore, the cell mortality obtained after irradiation of the cultures treated with the fullerenes was due to the photosensitization effect of the agent produced by visible light. The viability of *S. aureus* cells after irradiation was dependent upon both fullerene derivative used in the treatment and the light exposure level. First, cultures of ~$10^6$ CFU/mL were irradiated in culture tubes (13 × 100 mm) with visible light (Fig. 7). Similar photoinactivation for both fullerenes was obtained at shorter irradiation times. When the irradiation time was extended to 30 min, a higher photosensitizing activity was achieved for $DPC_{60}^{2+}$. The dicationic fullerene produced a 4.5 log decrease of cell survival, generating a 99.99% of cellular inactivation, while the non-charged fullerene showed an inactivation effect of 2.2 log

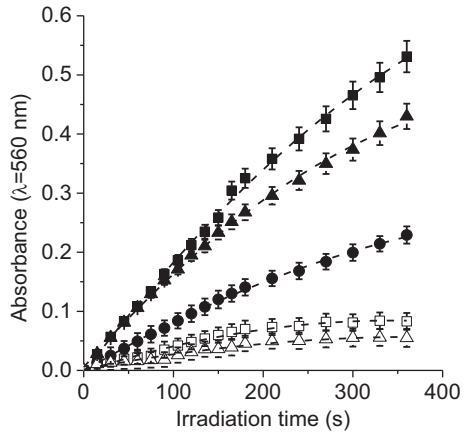


**Fig. 5.** Time course of $O_2^{\bullet-}$ generation detected by the NBT method as an increase in the absorption at 560 nm, for NBT + β-NADH (●); NBT + $MPC_{60}$ (□); NBT + $DPC_{60}^{2+}$ (△); NBT + β-NADH+ $MPC_{60}$ (■) NBT + β-NADH + $DPC_{60}^{2+}$ (▲) in DMF irradiated with visible light, [NBT] = 0.2 mM and [NADH] = 0.5 mM. Values represent mean ± standard deviation of three separate experiments.

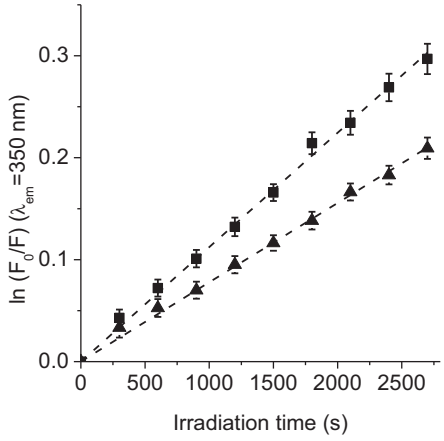


**Fig. 6.** First-order plots for the photooxidation of Trp (20 μM, $\lambda_{irr}$ = 450 nm) photosensitized by $MPC_{60}$ (■) and $DPC_{60}^{2+}$ (▲) in DMF. Values represent mean ± standard deviation of three separate experiments.

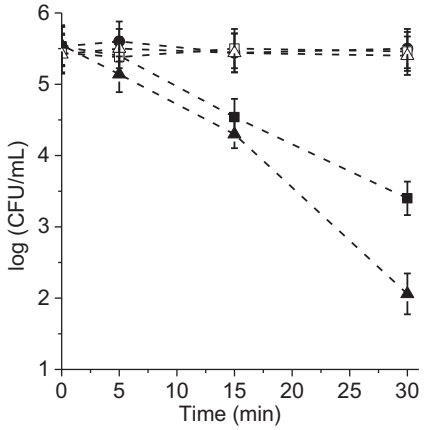


**Fig. 7.** Survival curves of *S. aureus* cells (2 mL, ~$10^6$ CFU/mL) incubated with 0.5 μM of $MPC_{60}$ (■) and $DPC_{60}^{2+}$ (▲) for 30 min at 37 °C in dark and exposed to visible light for different irradiation times in culture tubes (13 × 100 mm). Control cultures: cells treated with 0.5 μM $MPC_{60}$ (□) and $DPC_{60}^{2+}$ (△) in dark; cells untreated with the photosensitizer and irradiated (●). Values represent mean ± standard deviation of three separate experiments.

decrease. Moreover, the photodynamic activity of both fullerenes was evaluated irradiating ~$10^8$ CFU/mL *S. aureus* suspensions in 96-well microtiter plates (Fig. 8). This procedure was selected at a higher cell density because opaque suspensions were obtained with $10^8$ CFU/mL in culture tubes. This effect can produce a decrease in the cell photoinactivation because light did not penetrate deep enough into the suspension to activate the photosensitizer into the cells [35]. At this cellular density, the photocytotoxic activity mediated by both fullerenes was similar after 15 min irradiation, producing a ~4 log decrease of inactivation that signifies a 99.99% cell death. After 30 min irradiation, the cells treated with cationic fullerene $DPC_{60}^{2+}$ exhibited a decrease in cell survival of 4.8 log. This result represents a value greater than 99.998% of cell inactivation. Under the same conditions, $MPC_{60}$ evidenced a decay of 4.2 log in *S. aureus* inactivation. Thus, for both photosensitizers a decrease in susceptibility was observed in Fig. 8 with increasing time of PDI application. In the first part of the survival curve (<15 min), the population of more susceptible bacteria were faster photoinactivated. After this time, the remaining cells were less affected by photodamage and therefore, more difficult to eradicate. Also, photoinactivation of *S. aureus* induced by $DPC_{60}^{2+}$ was significantly higher than $MPC_{60}$, indicated that the presence of intrinsic positive charges in $DPC_{60}^{2+}$ produced a higher interaction with cells in comparison with its homologue containing amino groups.

Also, photoinactivation of *S. aureus* was examined in presence of 4.5% w/w bovine serum albumin (BSA), which represents the amount of this protein in blood plasma [36]. Albumin was chosen as a model since wound fluids can be mainly serum derived. In presence of this protein, a decrease in the phototoxicity sensitized by $DPC_{60}^{2+}$ was found producing a 62% inactivation after 30 min irradiation. Thus, the degree of microbial PDI depended on the BSA content of the cell suspension. The presence of serum albumin in the medium can reduce the amount of $DPC_{60}^{2+}$ bound to *S. aureus* due to the competitive interaction of the photosensitizer with the proteins.

Direct comparisons with other fullerenes already described are difficult mainly due to different experimental conditions. Effective dicationic fullerenes were previously investigated to photoinactivate *S. aureus* producing 4–6 logs decrease in cell survival [9,11]. Moreover, in the present work the photoinactivation activity mediated by $MPC_{60}$ was also effective. The photoinactivation capacity of $MPC_{60}$ can be compared with that produced by *N*, *N*-dimethyl-2-(4′-acetamidophenyl)fulleropyrrolidinium ($DAC_{60}^{+}$) [37]. Thus, it was found that $DAC_{60}^{+}$ induced only 1 log decrease, which was considerably lower than that of $MPC_{60}$, when *S. aureus* suspensions (~$10^6$ CFU/mL) were treated with 1 μM photosensitizer after 30 min irradiation. Even when $MPC_{60}$ not has intrinsic charge, the basic amino group of this fulleropyrrolidine derivative can be protonated at physiological pH, increasing the photodynamic activity against *S. aureus*.

## 4. Conclusions

A fulleropyrrolidine $MPC_{60}$, containing a basic amino group in the periphery of $C_{60}$ sphere, was synthetized by 1,3-dipotar cycloadditon of azomethine ylides to $C_{60}$ with 43% yield. Exhaustive methylation was used to obtain its dicationic analog yielding 96 % of $DPC_{60}^{2+}$. This basis amine group in $MPC_{60}$ can be protonated acquire positive charges depending on the medium. Also, this cationic center is isolated from the fullerene by a propoxy bridge, which provides a high mobility to the charge. A high photodynamic activity of these fullerenes was found in DMF and AOT reverse micelles. Generation of $O_2(^1\Delta_g)$ photosensitized by $MPC_{60}$ was higher than $DPC_{60}^{2+}$. Moreover, both fullerenes produced $O_2^{\bullet-}$ in presence of NADH and they are efficient

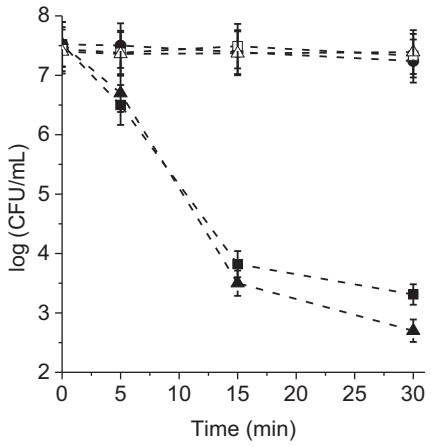


**Fig. 8.** Survival curves of *S. aureus* cells (0.2 mL, ~$10^8$ CFU/mL) incubated with 0.5 μM of $MPC_{60}$ (■) and $DPC_{60}^{2+}$ (▲) for 30 min at 37 °C in dark and exposed to visible light for different irradiation times in 96-well microtiter plates. Control cultures: cells treated with 0.5 μM $MPC_{60}$ (□) and $DPC_{60}^{2+}$ (△) kept in dark; cells untreated with the photosensitizer and irradiated (●). Values represent mean ± standard deviation of three separate experiments.

photosensitizers to decompose Trp with a possible involvement of type I photoprocess. *In vitro* studies showed that $DPC_{60}^{2+}$ was more active than $MPC_{60}$ to photosensitizer to photoinactivate *S. aureus* cells. Therefore, $DPC_{60}^{2+}$ can be used as effective photosensitizers with potential applications in microbial cell photoinactivation.

## Acknowledgements

Authors are grateful to Consejo Nacional de Investigaciones Científicas y Técnicas (CONICET, PIP 112-201101-00256) of Argentina, SECYT Universidad Nacional de Río Cuarto (PPI 18/C400) and Agencia Nacional de Promoción Científica y Tecnológica (FONCYT, PICT 0714) for financial support. M.B.S. M. E.M. and E.N.D. are Scientific Members of CONICET. M.L.A. and N.S. G. thank to CONICET for the research fellowships.

## Appendix A. Supplementary data

Supplementary data associated with this article can be found, in the online version, at http://dx.doi.org/10.1016/j.jphotochem.2015.05.022.

## References

[1] F.R. DeLeo, M. Otto, B.N. Kreiswirth, H.F. Chambers, Community-associated meticillin-resistant Staphylococcus aureus, Lancet 375 (2010) 1557–1568.
[2] H.F. Chambers, F.R. DeLeo, Waves of resistance: *Staphylococcus aureus* in the antibiotic era, Nat. Rev. Microbiol. 7 (2009) 629–641.
[3] A. Nigam, D. Gupta, A. Sharma, Treatment of infectious disease: beyond antibiotics, Microbiol. Res. 169 (2014) 643–651.
[4] E. Alves, M.A.F. Faustino, M.G.P.M.S. Neves, A. Cunha, J. Tome, A. Almeida, An insight on bacterial cellular targets of photodynamic inactivation, Fut. Med. Chem. 6 (2014) 141–164.
[5] T. Daia, Y.-Y. Huanga, M.R. Hamblin, Photodynamic therapy for localized infections-state of the art, Photodiagn. Photodyn. Ther. 6 (2009) 170–188.
[6] M.E. Milanesio, E.N. Durantini, Fullerene derivatives as antimicrobial photosensitising agents, in: M.R. Hamblin, G. Jori (Eds.), Comprehensive Series in Photodynamic Inactivation of Microbial Pathogens: Medical and Environmental Applications, Royal Society of Chemistry, Cambridge, 2011, pp. 161–184.
[7] S.K. Sharma, L.Y. Chiang, M.R. Hamblin, Photodynamic therapy with fullerenes *in vivo*: reality or a dream, Nanomedicine 6 (2011) 1813–1825.
[8] S. Bosi, T. Da Ros, G. Spalluto, M. Prato, Fullerene derivatives: an attractive tool for biological applications, Eur. J. Med. Chem. 38 (2003) 913–923.
[9] G.P. Tegos, T.N. Demidova, D. Arcila-Lopez, H. Lee, T. Wharton, H. Gali, M.R. Hamblin, Cationic fullerenes are effective and selective antimicrobial photosensitizers, Chem. Biol. 12 (2005) 1127–1135.
[10] M.B. Spesia, M.E. Milanesio, E.N. Durantini, Synthesis, properties and photodynamic inactivation of Escherichia coli by novel cationic fullerene $C_{60}$ derivatives, Eur. J. Med. Chem. 43 (2008) 853–861.
[11] L. Huang, M. Terakawa, T. Zhiyentayev, Y.-Y. Huang, Y. Sawayama, A. Jahnke, G.P. Tegos, T. Wharton, M.R. Hamblin, Innovative cationic fullerenes as broad-spectrum light-activated antimicrobials, Nanomed.: Nanotech. Biol. Med. 6 (2010) 442–452.
[12] M.E. Milanesio, M.B. Spesia, M.P. Cormick, E.N. Durantini, Mechanistic studies on the photodynamic effect induced by a dicationic fullerene $C_{60}$ derivative on Escherichia coli and *Candida albicans* cells, Photodiag. Photodyn. Ther. 10 (2013) 320–327.
[13] J. Mora, M.E. Milanesio, E.N. Durantini, Spectroscopic and photodynamic properties of 5,10,15,20-tetrakis[4-(3-*N*,*N*-dimethylaminopropoxy)phenyl] porphyrin and its tetracationic derivative in different media, J. Photochem. Photobiol. A: Chem. 270 (2013) 75–84.
[14] M. Novaira, M.P. Cormick, E.N. Durantini, Spectroscopic and time-resolved fluorescence emission properties of a cationic and an anionic porphyrin in biomimetic media and *Candida albicans* cells, J. Photochem. Photobiol. A: Chem. 246 (2012) 67–74.
[15] R. Hung, J. Grabowski, A precise determination of the triplet energy of $C_{60}$ by photoacoustic calorimetry, J. Phys. Chem. 95 (1991) 6073–6075.
[16] T. Hamano, K. Okuda, T. Mashino, M. Hirobe, K. Arakane, A. Ryu, S. Mashiko, T. Nagano, Singlet oxygen production from fullerene derivatives: effect of sequential functionalization of the fullerene core, J. Chem. Soc. Chem. Commun. (1997) 21–22.
[17] Y. Yamakoshi, N. Umezawa, A. Ryu, K. Arakane, N. Miyata, Y. Goda, T. Masumizu, T. Nagano, Active oxygen species generated from photoexcited fullerene ($C_{60}$) as potential medicines: $O_2^{\bullet-}$ versus $^1O_2$, J. Am. Chem. Soc. 125 (2003) 12803–12809.
[18] M. Ikeda, T. Akiyama, Photodynamic activity of liposomal photosensitizers via energy transfer from antenna molecules to [60] fullerene, ACS Med. Chem. Lett. 1 (2010) 115–119.
[19] M. Maggini, G. Scorrano, M. Prato, Addition of azomethine ylides to $C_{60}$: synthesis, characterization, and functionalization of fullerene pyrrolidines, J. Am. Chem. Soc. 115 (1993) 9798–9799.
[20] K.G. Thomas, V. Biju, M.V. George, D.M. Guldi, P.V. Kamat, Excited state interactions in pyrrolidinofullerenes, J. Phys. Chem. A 102 (1998) 5341–5348.
[21] D.M. Guldi, M. Prato, Excited-state properties of $C_{60}$ fullerene derivatives, Acc. Chem. Res. 33 (2000) 695–703.
[22] J.-F. Eckert, J.-F. Nicoud, J.-F. Nierengarten, S.-G. Liu, L. Echegoyen, F. Barigelletti, N. Armaroli, L. Ouali, V. Krasnikov, G. Hadziioannou, Fullerene-oligophenylenevinylene hybrids: synthesis, electronic properties, and incorporation in photovoltaic devices, J. Am. Chem. Soc. 122 (2000) 7467–7479.
[23] Y.-P. Sun, P. Wang, N.B. Hamilton, Fluorescence spectra and quantum yields of buckminsterfullerene ($C_{60}$) in room-temperature solutions. No excitation wavelength dependence, J. Am. Chem. Soc. 115 (1993) 6378–6381.
[24] D.M. Guldi, M. Maggini, G. Scorrano, M. Prato, Intramolecular electron transfer in fullerene/ferrocene based donor-bridge-acceptor dyads, J. Am. Chem. Soc. 119 (1997) 974–980.
[25] A. Gomes, E. Fernandes, J.L.F.C. Lima, Fluorescence probes used for detection of reactive oxygen species, J. Biochem. Biophys. Methods 65 (2005) 45–80.
[26] A.L. Ochoa, T.C. Tempesti, M.B. Spesia, M.E. Milanesio, E.N. Durantini, Eur. J. Med. Chem. 50 (2012) 280–287.
[27] F. Wilkinson, W.P. Helman, A.B. Ross, Rate constants for the decay and reactions of the lowest electronically excited singlet state of molecular oxygen in solution. An expanded and revised compilation, J. Phys. Chem. Ref. Data 24 (1995) 663–1021.
[28] J.M. Wessels, C.S. Foote, W.E. Ford, M.A.J. Rodgers, Photooxidation of tryptophan: $O_2(^1{}_g)$ versus electron-transfer pathway, Photochem. Photobiol. 65 (1997) 96–102.
[29] M.G. Milanesio, E.I. Alvarez, C.D. Yslas, J.J. Borsarelli, V. Silber, Photodynamic studies of metallo 5,10,15,20-tetrakis(4-methoxyphenyl) porphyrin: photochemical characterization and biological consequences in a human carcinoma cell line, Photochem. Photobiol. 74 (2001) 14–21.
[30] M.E. Daraio, A. Völker, P.F. Aramendia, E. San Roman, Tryptophan quenching of zinc-phthalocyanine and porphycene fluorescence in micellar CTAC, Photochem. Photobiol. 67 (1998) 371–377.
[31] V.S. Chirvony, V.A. Galievsky, N.N. Kruk, B.M. Dzhagarov, P.-Y. Turpin, Photophysics of cationic 5,10,15,20-tetrakis-(4-*N*-methylpyridyl) porphyrin bound to DNA, [poly(dA-dT)]2 and [poly(dG-dC)]2: on a possible charge transfer process between guanine and porphyrin in its excited singlet state, J. Photochem. Photobiol. B: Biol. 40 (1997) 154–162.
[32] M.E. Milanesio, M.G. Alvarez, J.J. Silber, V. Rivarola, E.N. Durantini, Photodynamic activity of monocationic and non-charged methoxyphenyl porphyrin derivatives in homogeneous and biological medium, Photochem. Photobiol. Sci. 2 (2003) 926–933.
[33] M.E. Milanesio, M.G. Alvarez, V. Rivarola, J.J. Silber, E.N. Durantini, Porphyrin-fullerene $C_{60}$ dyads with high ability to form photoinduced charge-separated state as novel sensitizers for photodynamic therapy, Photochem. Photobiol. 81 (2005) 891–897.
[34] T. Mashino, N. Usui, K. Okuda, T. Hirota, M. Mochizuki, Respiratory chain inhibition by fullerene derivatives: hydrogen peroxide production caused by fullerene derivatives and a respiratory chain system, Bioorg. Med. Chem. 11 (2003) 1433–1438.
[35] M.A. Di Palma, M.G. Alvarez, A.L. Ochoa, M.E. Milanesio, E.N. Durantini, Optimization of cellular uptake of zinc(II) 2,9,16,23-tetrakis[4-(*N*-

methylpyridyloxy)]phthalocyanine for maximal photoinactivation of *Candida albicans*, Fungal Biol. 117 (2013) 744–751.

[36] S.A.G. Lambrechts, M.C.G. Aalders, F.D. Verbraak, J.W.M. Lagerberg, J.B. Dankert, J.J. Schuitmaker, Effect of albumin on the photodynamic inactivation of microorganisms by a cationic porphyrin, J. Photochem. Photobiol B: Biol. 79 (2005) 51–57.

[37] M.B. Ballatore, M.B. Spesia, M.E. Milanesio, E.N. Durantini, Synthesis, spectroscopic properties and photodynamic activity of porphyrin-fullerene $C_{60}$ dyads with application in the photodynamic inactivation of *Staphylococcus aureus*, Eur. J. Med. Chem. 83 (2014) 685–694.